Molecular & Cellular Toxicology (2024) 20:315–323
https://doi.org/10.1007/s13273-023-00345-2

ORIGINAL ARTICLE

STYXL1 promotes proliferation and epithelial mesenchymal transition of gastric cancer cells via activating the PI3K/AKT pathway

Silu Chen[1] · Weiyan Yu[2] · Ziyue Li[2] · Yadong Wang[2] · Bo Peng[1]

Accepted: 23 February 2023 / Published online: 10 March 2023

Abstract

Background Gastric cancer (GC) is a common and grievous disorder with high heterogeneity. Serine/threonine/tyrosine-interacting-like protein 1 (STYXL1), a pseudophosphatase without catalytic activity, plays a important roles in cellular pathways and various cancers. However, its role and mechanism in GC remain unclear.

Objectives This study aimed to explore the role and possible mechanism of STYXL1 in GC cells.

Results The results showed that STYXL1 expression was elevated in GC. Both loss- and gain-of-function results showed that STYXL1 enhanced cell viability, colony formation, cell invasion and migration, and the protein expression of BCL-2 and Vimentin, but reduced the apoptosis rate and the protein level of BAX, cleaved caspase 3 and E-Cadherin in vitro. Mechanically, the levels of p-PI3K/PI3K and p-AKT/AKT were observably elevated by overexpression of STYXL1, and markedly reduced by silencing of STYXL1 in both SNU-1 and HGC-27 cells.

Conclusion STYXL1 promoted cell growth, migration, invasion and EMT with decreased apoptosis, which was closely related with the activation of PI3K/AKT pathway in GC.

Keywords Gastric cancer · STYXL1 · Proliferation · Epithelial mesenchymal transition · PI3K/AKT

Introduction

Gastric cancer (GC) is the fifth most common cancer and the third most common cause for cancer death, with more than 1 million new cases and 768 793 consequential deaths in 2020 all over the world (Smyth et al. 2020). Multiple causes have been identified as risk factors for GC, including *Helicobacter pylori* infection, high salt uptake, age, and diets low in vegetables and fruit (Lordick et al. 2022). The intervenes for GC include endoscopic resection for early GC, surgery for non-early operable GC, perioperative or adjuvant chemotherapy for stage 1B or higher GC, and sequential lines of chemotherapy for advanced gastric (Smyth et al. 2020). The vast majority of GC patients were in advanced stages when they are first diagnosed due to the asymptomatic nature of GC in the early stages, which makes about two-thirds of GC patients face incurable, eventually resulting in a less than one-thirds GC patients surviving beyond five years (den Hoed and Kuipers 2016; Lordick et al. 2022). Moreover, potent metastasis also contributes to the poor prognosis of GC patients (Peng et al. 2018). Thus, in-depth comprehension of the mechanism and process of GC can better boost the development of clinical diagnosis and treatment of GC.

Serine/threonine/tyrosine-interacting-like protein 1 (STYXL1), also known as mitogen-activated protein kinase phosphoserine/threonine/tyrosine-binding protein (MK-STYX), is a pseudophosphatase, belonging to the protein tyrosine phosphatase (PTP) superfamily without catalytic activity due to the replacement of histidine and cysteine residues with phenylalanine and serine residues (FSTQGISR) in its PTP active site signature motif (HCX5R) (Hinton 2019; Hinton et al. 2010; Tonks 2006; Wishart et al. 1998). Despite of the absence of catalytic property, STYXL1 has been revealed to regulate a series of cellular pathways, such as mitochondrially dependent apoptosis (Niemi et al. 2011), stress granule assembly (Barr et al. 2013), localization and

✉ Bo Peng
bo_p999@163.com

[1] Department of Gastroenterology, Wuhan Third Hospital, Tongren Hospital of Wuhan University, No. 216, Guanshan Avenue, Hongshan District, Wuhan 430060, Hubei Province, China

[2] Department of Infectious Diseases, The Third Affiliated Hospital of Hebei Medical University, Shijiazhuang 050000, Hebei Province, China

phosphorylation of histone deacetylase 6 (Cao, et al. 2019), the morphology of primary neurons (Banks et al. 2017), neuronal differentiation (Flowers et al. 2014) and intellectual disability, epilepsy and behavioural complexities (Isrie et al. 2015). In addition, the important role of STYXL1 has been demonstrated in different tumors, including Ewing's sarcoma family tumors (Siligan et al. 2005), prostate cancer (Winter et al. 2018), hepatocellular carcinoma (Wu et al. 2020) and glioblastoma (Tomar et al. 2019). Nevertheless, the role of STYXL1 in GC is still undiscovered.

Therefore, the role and possible mechanism of STYXL1 were explored in GC cells. Firstly, the STYXL1 level was detected in GC cells. Then, the role of STYXL1 in growth, apoptosis, mobility, invasion and epithelial-mesenchymal transition (EMT) of GC cells was explored in both HGC-27 and SNU-1 cells through loss- and gain-of-function examinations. Finally, the potential mechanism of STYXL1 in the GC progression was investigated in both cells by examining the expression of proteins involved in the PI3K/AKT axis.

Materials and methods

Public database analysis

The STYXL1 expression in stomach adenocarcinoma (STAD) samples and normal tissue samples (para-carcinoma samples) was analyzed through the UALCAN (http://ualcan.path.uab.edu/index.html), a comprehensive resource from TCGA database. The overall survival was constructed via the kmplot database (http://kmplot.com/).

Cell culture

Human gastric mucosal cell line GES-1 (CL-0563), and GC cell lines, including NCI-N87 (CL-0169) and HGC-27 (CL-0107) were obtained from Prrocell (Wuhan, China), while GC cells SNU-1 (CRL-5971) were bought from American Type Culture Collection (ATCC, Manassas, VA). All cells were cultured in RPMI-1640 (PM150110, Procell) provided with 10% fetal bovine serum (FBS, 12103 C, Merck, Whitehouse Station, NJ, USA) and 1% streptomycin-penicillin (P/S, PB180120, Procell) in an incubator with 5% CO_2 at 37 °C.

Cell transfection

The short hairpin RNAs (shRNA) against STYXL1 (shSTYXL1) and the corresponding negative control (shNC) packed into lentivirus, as well as the overexpressing lentivirus of STYXL1 (STYXL1) and the relevant NC (Control) were prepared from Genechem (Shanghai, China). The interfering and overexpressing lentivirus of STYXL1 were infected into SNU-1 and HGC-27 cells according to the operating manual from the company.

Cell counting kit-8 (CCK-8) assay

Cells were plated into 96-well plates with an inoculation density of 2×10^3 cells/well. The cell viability of both cells was detected with a CCK-8 Cell Proliferation and Cytotoxicity Assay Kit (CA1210, Solarbio, Beijing, China) based on the operation instruction.

Colony formation assay

HGC-27 and SNU-1 cells were mixed in 2 ml of RPMI-1640 including 10% FBS and inoculated into 6-well plates with the 500 cells/well. Next, both cells were cultured at 37 °C for two weeks, and then fixed with 4% paraformaldehyde (P1110, Solarbio) for half an hour and stained with 0.1% crystal violet (G1063, Solarbio) for half an hour. The colonies were manually enumerated and photographed.

Analysis of apoptosis rate

The apoptosis of HGC-27 and SNU-1 cells was assessed by flow cytometry as the previous descriptions (Yang et al. 2022). In brief, after being gathered and immobilized with 70% ethanol for one day at -30 °C, both cells were stained with 5 μL Annexin V-FITC and propidium iodide (PI) (CA1020, Solarbio) without light at room temperature for 5 min. The results were evaluated on a FACScan flow cytometer with the CellQuest software (BD Biosciences, NJ, USA).

Transwell assays

The mobility and invasion of both cells were evaluated by transwell assay as the previous reported (Lee et al. 2022). Briefly, cells with a density of 5×10^4 cells/well were plated into the upper cabinet of 24-well transwell plates with an 8-μm pore size (3422, Corning Company, New York, NY, USA), and RPMI-1640 media with 10% FBS were filled into the lower chamber. Following the incubation, both cells transferred to the lower chamber were fixed with methanol and stained with 0.1% crystal violet (G1063, Solarbio) for half an hour. The operation of the invasion experiment was consistent with the migration assay as above-mentioned protocol, except that the upper cabinet of transwell plates was enveloped with Matrigel (356,234, Solarbio). Cells were pictured and analyzed for the ability of migration and invasion.

Western blot

The assays were performed as the previous methods (Chhabra et al. 2021; Lee et al. 2022). Proteins from HGC-27 and SNU-1 cells were extracted with the RIPA buffer (R0010, Solarbio) and centrifuged for 5 min at 12,000 g for the collection of the supernatant. Total proteins were quantified with BCA kit (PC0020, Solarbio). 20 μg proteins were separated with 10% sodium dodecyl-sulfate polyacrylamide gel electrophoresis (SDS-PAGE) and electrically transferred onto PVDF membranes (IPVH00010, Millipore, Billerica, MA, USA). The membranes were treated with 5% BSA Blocking Buffer (SW3015, Solarbio) at room temperature for 2 h for the blocking and with primary antibodies targeting STYXL1 (ab67913, 1:1000), BAX (ab104156, 1:1000), BCL2 (ab196495, 1:2000), cleaved caspase 3 (ab2302, 1:500), E-Cadherin (ab40772, 1:50,000), Vimentin (ab92547, 1:5000), phosphorylated PI3K (p-PI3K) (ab278545, 1:2000), PI3K (ab180967, 1:500), p-AKT (ab38449, 1:2000), AKT (ab8805, 1:1000) and anti-β-actin (1:5000, ab8227) were added into membranes for overnight at 4 °C. After incubated with the goat anti-mouse IgG H&L (HRP) (ab6789, 1:10,000) or goat anti-rabbit IgG H&L (HRP) (ab6721, 1:10,000), the bands were exposed with ECL Western Blotting Substrate (PE0010, Solarbio). The band intensity was analyzed by QUANTITY ONE software (Bio-Rad, Hercules, CA, USA). All antibodies were from Abcam (Cambridge, UK).

Statistical analysis

All data were expressed as mean ± standard deviation (SD) and analyzed by SPSS 20.0 software (IBM, Armonk, New York, USA). Statistical differences were detected with the Student's *t* test (only two groups) or one-way analysis of variance (ANOVA) (more than two groups) followed by Post Hoc Bonferroni test. $P < 0.05$ was defined as significant difference.

Results

STYXL1 was upregulated in GC

To explore the role of STYXL1 in GC, the STYXL1 level was first examined in GC. The data from the UALCAN database displayed that the STYXL1 expression was enhanced in GC samples compared with normal samples (Fig. 1A). Moreover, upregulation of STYXL1 predicted anpoor survival in GC patients (Fig. 1B). The levels of STYXL1 were also significantly increased in GC cell lines, including SNU-1, HGC-27 and NCI-N87 cells compared with human gastric mucosal cell line GES-1, among which the STYXL1 level in SNU-1 and HGC-27 cells was higher than that in NCI-N87 cells (Fig. 1C). Thus, the first two cells were employed in the following assays. Altogether, upregulated expression of STYXL1 in GC predicted an unfavorable survival in GC patients.

Downregulation of STYXL1 restrained GC cell growth

To address the action of STYXL1 in the GC progression, the level of STYXL1 was effectively overexpressed and interfered in both SNU-1 and HGC-27 cells, respectively (Fig. 2A). The cell viability and numbers of colonies were significantly elevated in both cells overexpressed with STYXL1 compared with these in control group (Fig. 2B, C). On the contrary, knockdown of STYXL1 prominently reduced the cell viability and numbers of colonies in both cells compared with these in shNC group (Fig. 2 B, C). Thus, downregulation of STYXL1 suppressed the growth of GC.

Silencing of STYXL1 promoted apoptosis in GC cells

Then, the role of STYXL1 in cell apoptosis was investigated in GC cells. The apoptosis rate was observably declined after both cells were overexpressed with STYXL1, while a prominent enhancement of apoptosis rate was observed in both cells downregulated with STYXL1 (Fig. 3A). In addition, overexpression of STYXL1 markedly decreased the protein level of BAX and cleaved caspase 3, whereas augmented the protein expression of BCL-2 in both cells (Fig. 3B). Nevertheless, interference of STYXL1 notably elevated the protein expression of BAX and cleaved caspase 3 and decreased the protein expression of BCL-2 in cells (Fig. 3B). Therefore, knockdown of STYXL1 enhanced apoptosis in GC cells.

Interference of STYXL1 restrained mobility, invasion and EMT of GC cells

Next, the role of STYXL1 in migration, invasion and EMT was explored in both SNU-1 and HGC-27 cells. Overexpression of STYXL1 significantly augmented the numbers of invasive and migrated cells, but downregulation of STYXL1 had opposite effects in both cells (Fig. 4A). Meanwhile, overexpression of STYXL1 prominently reduced the E-Cadherin expression but enhanced the Vimentin expression of in both cells (Fig. 4B). On the other hand, knockdown of STYXL1 notably elevated the E-Cadherin expression but diminished the Vimentin expression of in both cells (Fig. 4B). Hence, knockdown of STYXL1 attenuated migration, invasion and EMT of GC cells.

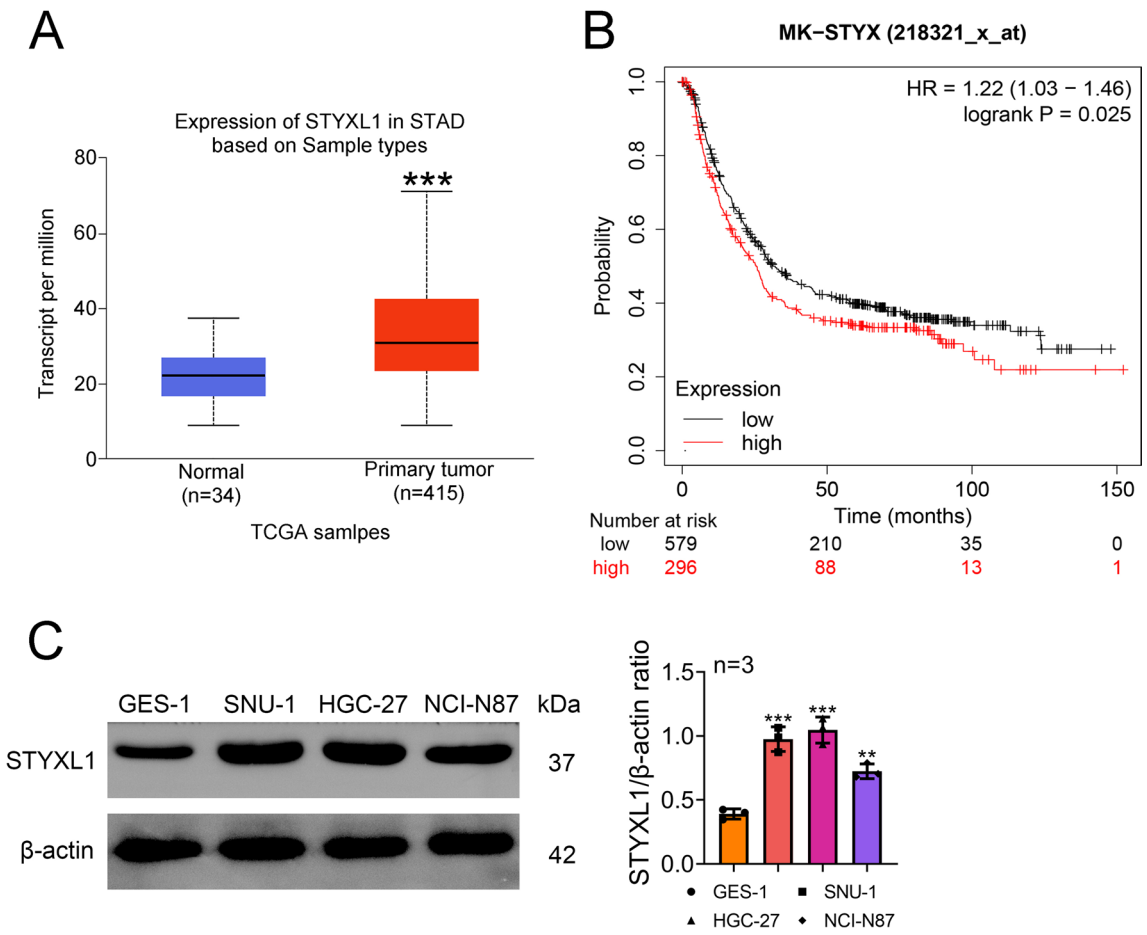

Fig. 1 The expression of STYXL1 was upregulated in GC, which predicted a poor survival in patients with GC. **A** Analysis of STYXL1 in GC through the UALCAN database. ***$P < 0.001$ *vs.* Normal. **B** Prediction of survival in patients with GC based on the STYXL1 expression. **C** The expression of STYXL1 was detected by western blot in human gastric mucosal cell line GES-1, as well as GC cell lines, including SNU-1, HGC-27 and NCI-N87 cells. Data were exhibited after normalized with -β-actin. **$P < 0.01$ and ***$P < 0.001$ *vs.* GES-1

STYXL1 activated the PI3K/AKT axis

Mechanically, the effects STYXL1 on the expression of proteins involved in PI3K/AKT axis was detected in both cells. Results from Fig. 5 revealed that the levels of p-PI3K/PI3K and p-AKT/AKT were observably elevated by overexpression of STYXL1, while they were markedly reduced by silencing of STYXL1 in both SNU-1 and HGC-27 cells. Thus, STYXL1 enhanced the level of the PI3K/AKT axis.

Discussion

STYXL1 is involved in the progression and development of diverse cancers, but its function and mechanism in GC remain unknown. Our result showed that the STYXL1 expression was augmented in GC. Both gain- and loss-of-function results showed that STYXL1 accelerated growth, mobility, invasion and EMT, but inhibited apoptosis in both SNU-1 and HGC-27 cells. Mechanically, STYXL1 activated the PI3K/AKT signaling. Totally, STYXL1 enhanced the development of GC through the activation of PI3K/AKT axis.

STYXL1 has been identified as biomarker in different disease models, such as late-onset major depressive disorder (Miyata et al. 2016) and diabetes mellitus (Elsherbini et al. 2022). Moreover, the expression of STYXL1 is reported to be upregulated in different cancers, such as prostate cancer (Winter et al. 2018), hepatocellular carcinoma (Wu et al. 2020) and glioblastoma (Tomar et al. 2019). Consistent to these results, the expression of STYXL1 in the current study was also increased in GC samples from the UALCAN database and GC cell lines, which indicated that STYXL1 might serve as a biomarker for the diagnosis and therapy of GC. Furthermore, upregulation of STYXL1 predicted an unfavourable survival in

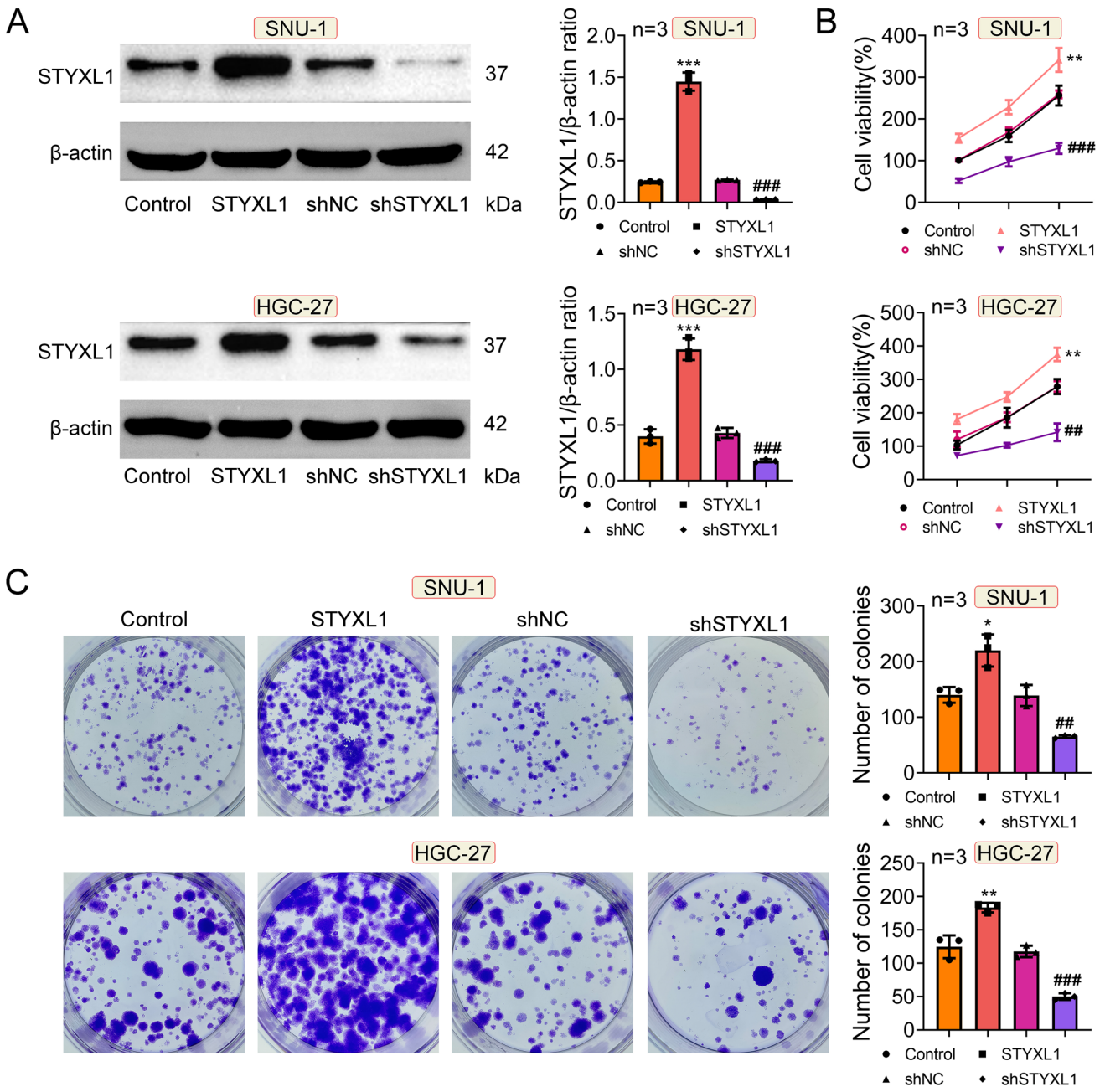

Fig. 2 Silencing of STYXL1 repressed the growth of GC. **A** The relative protein expression of STYXL1 was examined by western blot after SNU-1 and HGC-27 cells were overexpressed and interfered with STYXL1. Data were exhibited after normalized with β-actin. **B** The cell viability of both SNU-1 and HGC-27 cells was determined by CCK-8 assays. **C** The numbers of colonies were counted after SNU-1 and HGC-27 cells with different treatments were grown 37 °C for two weeks, immobilized with paraformaldehyde and stained with 0.1% crystal violet. $^{*}P<0.05$, $^{**}P<0.01$ and $^{***}P<0.001$ *vs.* Control; $^{\#\#}P<0.01$ and $^{\#\#\#}P<0.001$ *vs.* shNC

GC patients, which is similar to the poor prognosis in hepatocellular carcinoma (Wu et al. 2020) and glioblastoma (Tomar et al. 2019). In addition, STYXL1 expression is correlated to Gleason Score, tumor stage and nodal metastases in prostate cancer (Winter et al. 2018). Taken together, upregulated expression of STYXL1 in GC predicted a poor survival in patients with GC.

Proliferation, apoptosis, migration, invasion and EMT are pivotal progression of tumors, which have been acted as hallmarks of tumors (Hanahan 2022). STYXL1 has been demonstrated to be an oncogene due to the modulatory action in the progression of diverse tumors. For instance, STYXL1 contributes to the growth, mobility and invasion in glioblastoma (Tomar et al. 2019). STYXL1 promotes proliferation

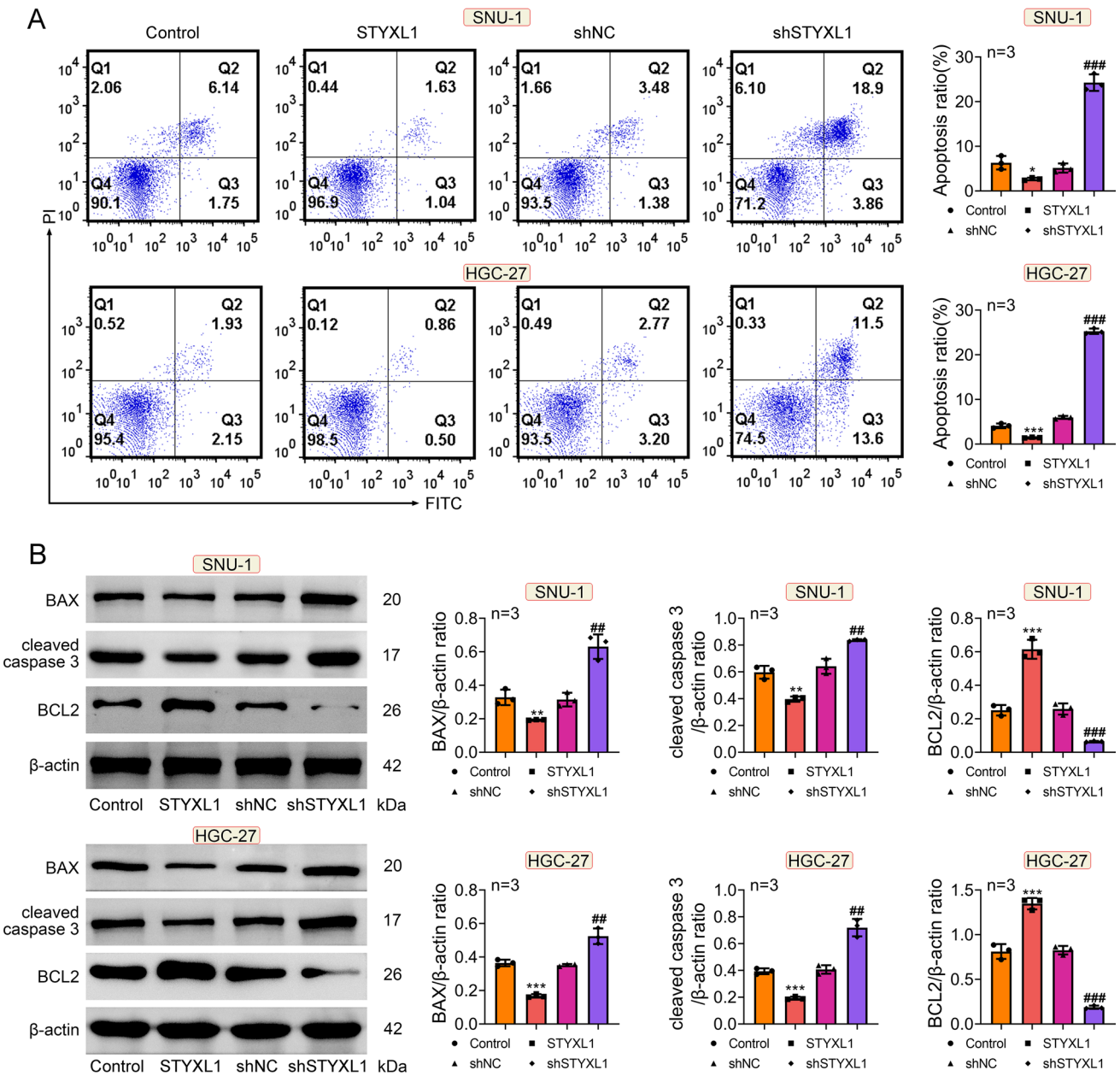

Fig. 3 Downregulation of STYXL1 facilitated apoptosis in GC cells. **A** The apoptosis rate was analyzed by flow cytometry after SNU-1 and HGC-27 cells were overexpressed and interfered with STYXL1. **B** The relative protein expression of BAX, cleaved caspase 3 and BCL-2 in both SNU-1 and HGC-27 cells was measured by western blot. Data were exhibited after normalized with β-actin. $^{*}P<0.05$, $^{**}P<0.01$ and $^{***}P<0.001$ *vs.* Control; $\#\#P<0.01$ and $\#\#\#P<0.001$ *vs.* shNC

and suppresses apoptosis of hepatocellular carcinoma cells (Wu et al. 2020). Moreover, STYXL1 also enhanced cell viability, numbers of colonies, numbers of invasive and migratory cells and the relative protein expression of BCL-2 and Vimentin, but reduced the apoptosis rate and the protein levels of BAX, cleaved caspase 3 and E-Cadherin in cells through both gain- and loss-of-function assays. BCL-2, BAX and cleaved caspase 3 are momentous components of apoptosis (Cassier et al. 2017), among which BCL-2 and BAX are pro-apoptosis gene and anti-apoptosis gene involved in the regulation of apoptosis (Edlich 2018), and cleaved caspase 3, the activated modality of caspase 3 associates with the different stages of apoptotic signaling (Asadi et al. 2021). Activation of EMT is a critical step of cancer cell metastasis, during which epithelial cells gain the characteristics of mesenchymal cells, and cell motility and migration ability are enhanced (Pastushenko et al. 2019). It has demonstrated that reduced E-cadherin causes the reduced adhesion and

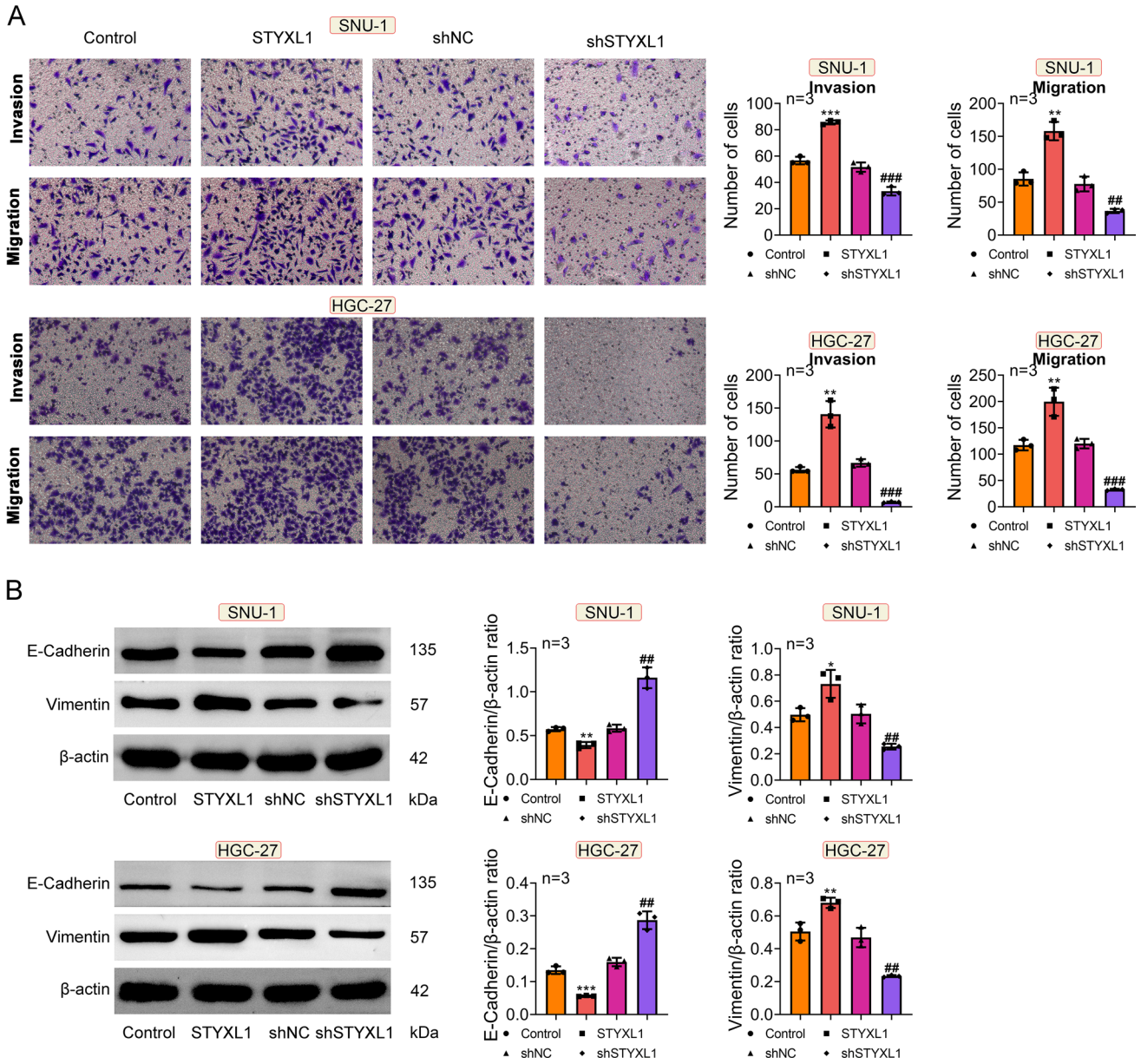

Fig. 4 Interference of STYXL1 suppressed migration, invasion and EMT of GC cells. **A** The numbers of invasive and migratory cells were counted by transwell assays. **B** The relative protein expression of E-Cadherin and Vimentin was detected by western blot. Data were exhibited after normalized with β-actin. $^{**}P<0.01$ and $^{***}P<0.001$ *vs.* Control; $\#\#P<0.01$ and $\#\#\#P<0.001$ *vs.* shNC

the elevation of invasion and mobility, and reverse outcomes are revealed for elevated Vimentin (Christiansen et al. 2006; Satelli et al. 2011; Wheelock et al. 2003). Therefore, elevation of Vimentin and diminishment of E-cadherin are the typical manifestation of EMT (Bai et al. 2020). Collectively, STYXL1 promoted growth, mobility, invasion and EMT, but inhibited apoptosis in GC cells.

PI3K/AKT axis is a classical signaling pathway intertwined with an extensive variety of physiological and pathological condition (Deng et al. 2021; Lee et al. 2022). The detailed role of PI3K/AKT pathway in the progression, resistance, metastasis and prognosis of GC has been recapitulated in the review by Fattahi et al. (Fattahi et al. 2020). Inhibitors for the PI3K/AKT signaling have been revealed to be potential approaches for the GC treatment (Fattahi et al. 2020). Here, the levels of p-PI3K/PI3K and p-AKT/AKT were observably elevated by overexpression of STYXL1, and was markedly reduced by silencing of STYXL1 in both SNU-1 and HGC-27 cells. The promotive role of STYXL1 in hepatocellular carcinoma is closely related to the PI3K/AKT axis, in which STYXL1 enhances the expressions of proteins associated with PI3K/

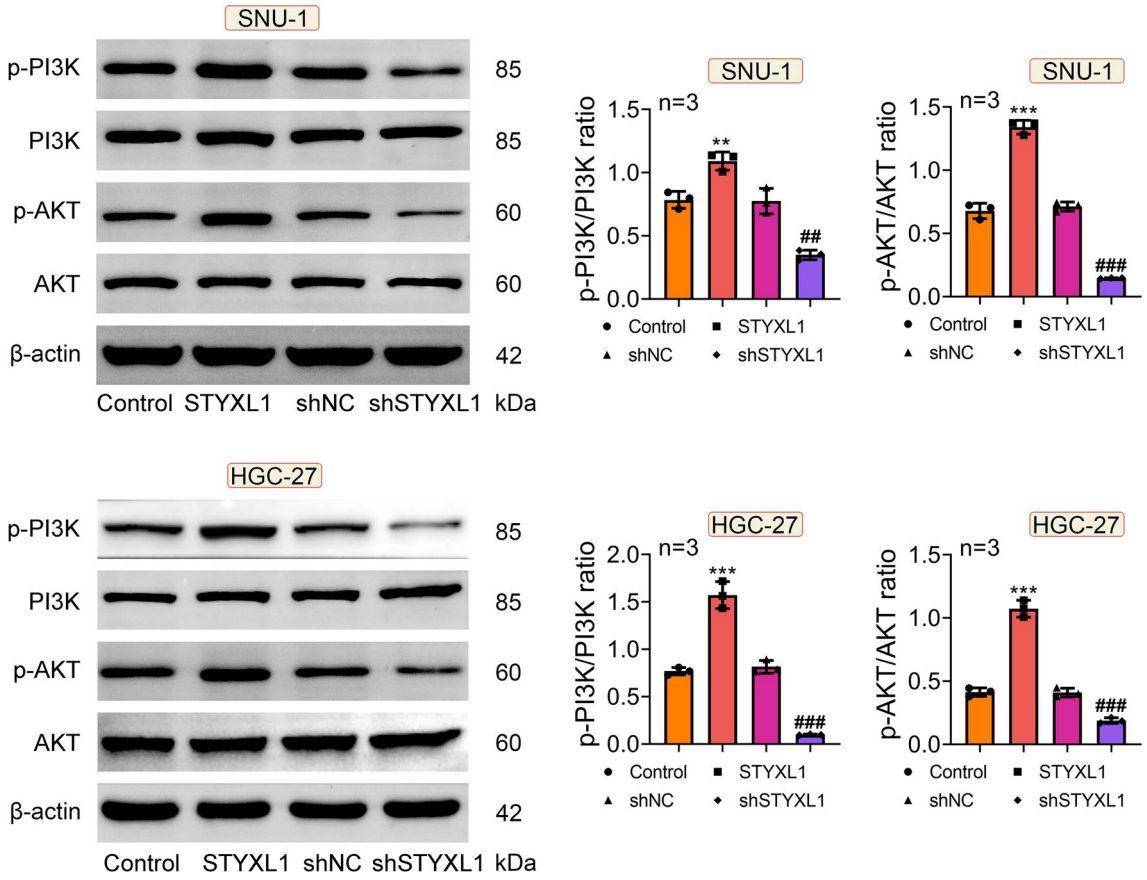

Fig. 5 STYXL1 promoted the expression of the PI3K/AKT signaling pathway. The relative protein expression of p-PI3K, PI3K, p-AKT and AKT was examined by western blot. Data were exhibited after normalized with β-actin. $^{**}P<0.01$ and $^{***}P<0.001$ *vs.* Control; $^{\#\#}P<0.01$ and $^{\#\#\#}P<0.001$ *vs.* shNC

AKT pathway (Wu et al. 2020). Therefore, these results indicated that the role of STYXL1 in the GC progression might be closely related to the activation of PI3K/AKT axis.

Conclusion

In summary, STYXL1 was upregulated in GC. Both gain- and loss-of-function results revealed that STYXL1 facilitated growth, mobility, invasion and EMT, but inhibited apoptosis in vivo, which might be related to the activation of PI3K/AKT axis. However, these are still limitations in this study. First, the direct role of PI3K/AKT axis should be examined through the pharmacological interference or other effective interventions in the following study. In addition, the role of STYXL1 in GC can be investigated in vivo. In conclusion, our results illuminate that STYXL1 has the potential to serve as a biomarker for the diagnosis and therapy of GC.

Author contributions SC and BP designed the experiments, SC, WY, ZL and YW carried them out, analyzed and interpreted the data, SC and BP prepared the manuscript. All authors have read and approved the manuscript.

Funding No funding was used in this study.

Data availability The authors declare that all data supporting the findings of this study are available within the paper and any raw data can be obtained from the corresponding author upon request.

Declarations

Conflict of interest Author Silu Chen declares that he/she has no conflict of interest; author Weiyan Yu declares that he/she has no conflict of interest; author Ziyue Li declares that he/she has no conflict of interest; author Yadong Wang declares that he/she has no conflict of interest; author B Bo Peng declares that he/she has no conflict of interest.

Ethical approval This article does not contain any studies with human participants or animals performed by any of the authors.

References

Asadi M et al (2021) Caspase-3: structure, function, and biotechnological aspects. Biotechnol Appl Biochem 11:435

Bai Y, Sha J, Kanno T (2020) The Role of carcinogenesis-related biomarkers in the wnt pathway and their effects on epithelial-mesenchymal transition (EMT) in oral squamous cell carcinoma. Cancers (basel) 12:876

Banks DA et al (2017) MK-STYX alters the morphology of primary neurons, and outgrowths in MK-STYX overexpressing PC-12 cells develop a neuronal phenotype. Front Mol Biosci 4:76

Barr JE, Munyikwa MR, Frazier EA, Hinton SD (2013) The pseudophosphatase MK-STYX inhibits stress granule assembly independently of Ser149 phosphorylation of G3BP-1. Febs j 280:273–284

Cao Y et al (2019) Pseudophosphatase MK-STYX alters histone deacetylase 6 cytoplasmic localization, decreases its phosphorylation, and increases detyrosination of tubulin. Int J Mol Sci 20:665

Cassier PA, Castets M, Belhabri A, Vey N (2017) Targeting apoptosis in acute myeloid leukaemia. Br J Cancer 117:1089–1098

Chhabra R et al (2021) Characterization of stem cells from human exfoliated deciduous anterior teeth with varying levels of root resorption. J Clin Pediatr Dent 45:104–111

Christiansen JJ, Rajasekaran AK (2006) Reassessing epithelial to mesenchymal transition as a prerequisite for carcinoma invasion and metastasis. Cancer Res 66:8319–8326

den Hoed CM, Kuipers EJ (2016) Gastric cancer: how can we reduce the incidence of this disease? Curr Gastroenterol Rep 18:34

Deng P et al (2021) Study on the molecular mechanism of Guizhi Jia Shaoyao decoction for the treatment of knee osteoarthritis by utilizing network pharmacology and molecular docking technology. Allergol Immunopathol (madr) 49:16–30

Edlich F (2018) BCL-2 proteins and apoptosis: Recent insights and unknowns. Biochem Biophys Res Commun 500:26–34

Elsherbini AM et al (2022) Decoding Diabetes Biomarkers and Related Molecular Mechanisms by Using Machine Learning, Text Mining, and Gene Expression Analysis. Int J Environ Res Public Health 19:769

Fattahi S et al (2020) PI3K/AKT/mTOR signaling in gastric cancer: Epigenetics and beyond. Life Sci 262:118513

Flowers BM et al (2014) The pseudophosphatase MK-STYX induces neurite-like outgrowths in PC12 cells. PLoS ONE 9:e114535

Hanahan D (2022) Hallmarks of cancer: new dimensions. Cancer Discov 12:31–46

Hinton SD (2019) The role of pseudophosphatases as signaling regulators. Biochim Biophys Acta Mol Cell Res 1866:167–174

Hinton SD et al (2010) The pseudophosphatase MK-STYX interacts with G3BP and decreases stress granule formation. Biochem J 427:349–357

Isrie M et al (2015) Homozygous missense mutation in STYXL1 associated with moderate intellectual disability, epilepsy and behavioural complexities. Eur J Med Genet 58:205–210

Lee EH et al (2022) Inhibition of TRPM7 suppresses migration and invasion of prostate cancer cells via inactivation of ERK1/2. Src and Akt Pathway Signal JOMH 18:345

Lordick F et al (2022) Gastric cancer: ESMO Clinical Practice Guideline for diagnosis, treatment and follow-up. Ann Oncol 33:1005–1020

Miyata S et al (2016) Blood Transcriptomic Markers in Patients with Late-Onset Major Depressive Disorder. PLoS ONE 11:e0150262

Niemi NM et al (2011) MK-STYX, a catalytically inactive phosphatase regulating mitochondrially dependent apoptosis. Mol Cell Biol 31:1357–1368

Pastushenko I, Blanpain C (2019) EMT Transition States during Tumor Progression and Metastasis. Trends Cell Biol 29:212–226

Peng L, Yu K, Li Y, Xiao W (2018) Gastric metastasis of recurrent hepatocellular carcinoma: A case report and literature review. J Cancer Res Ther 14:S1230-s1232

Satelli A, Li S (2011) Vimentin in cancer and its potential as a molecular target for cancer therapy. Cell Mol Life Sci 68:3033–3046

Siligan C et al (2005) EWS-FLI1 target genes recovered from Ewing's sarcoma chromatin. Oncogene 24:2512–2524

Smyth EC et al (2020) Gastric cancer. Lancet 396:635–648

Tomar VS, Baral TK, Nagavelu K, Somasundaram K (2019) Serine/threonine/tyrosine-interacting-like protein 1 (STYXL1), a pseudo phosphatase, promotes oncogenesis in glioma. Biochem Biophys Res Commun 515:241–247

Tonks NK (2006) Protein tyrosine phosphatases: from genes, to function, to disease. Nat Rev Mol Cell Biol 7:833–846

Wheelock MJ, Johnson KR (2003) Cadherins as modulators of cellular phenotype. Annu Rev Cell Dev Biol 19:207–235

Winter JM et al (2018) Modifier locus mapping of a transgenic F2 mouse population identifies CCDC115 as a novel aggressive prostate cancer modifier gene in humans. BMC Genomics 19:450

Wishart MJ, Dixon JE (1998) Gathering STYX: phosphatase-like form predicts functions for unique protein-interaction domains. Trends Biochem Sci 23:301–306

Wu JZ, Jiang N, Lin JM, Liu X (2020) STYXL1 promotes malignant progression of hepatocellular carcinoma via downregulating CELF2 through the PI3K/Akt pathway. Eur Rev Med Pharmacol Sci 24:2977–2985

Yang X, Gong J, Cai X, Yuan Y (2022) Overexpression of HIC1 plays a protective effect on renal cell injury caused by lipopolysaccharide by inhibiting IL-6/STAT3 pathway. Signa Vitae 18:147–153